



# Comparing attenuations of malignant and benign solitary pulmonary nodule using semi-automated region of interest selection on contrast-enhanced CT

Yangsean Choi<sup>1</sup>, Bo Mi Gil<sup>1</sup>, Myung Hee Chung<sup>1</sup>, Won Jong Yoo<sup>1</sup>, Na Young Jung<sup>1</sup>, Yong Hyun Kim<sup>2</sup>, Soon Seog Kwon<sup>2</sup>, Jeana Kim<sup>3</sup>

<sup>1</sup>Department of Radiology, <sup>2</sup>Division of Allergy and Pulmonary, Department of Internal Medicine, <sup>3</sup>Department of Hospital Pathology, Bucheon St. Mary's Hospital, College of Medicine, The Catholic University of Korea, Bucheon, Korea

**Contributions:** (I) Conception and design: MH Chung; (II) Administrative support: MH Chung, BM Gil; (III) Provision of study materials or patients: MH Chung; (IV) Collection and assembly of data: Y Choi, BM Gil; (V) Data analysis and interpretation: MH Chung, BM Gil; (VI) Manuscript writing: All authors; (VII) Final approval of manuscript: All authors.

**Correspondence to:** Bo Mi Gil, MD. Department of Radiology, Bucheon St. Mary's Hospital, College of Medicine, The Catholic University of Korea, 327, Sosa-ro, Bucheon-si, Gyeonggi-do 14647, Korea. Email: xhxhh@catholic.ac.kr.

**Background:** The purpose of this study was to determine whether semi-automated region of interest (ROI) measurement of CT attenuations of solitary pulmonary nodule (SPN) is an accurate approach in differentiating malignant from benign SPN.

**Methods:** Ninety cases of pathologically proven SPN were retrospectively reviewed. CT attenuations of SPN before and after contrast injection were measured using semi-automated ROI selection method. Attenuations within a range of -100 to 200 Hounsfield units (HU) as soft tissue density range were set. The ROI included the entire SPN regardless of its internal soft tissue contents after automatic elimination of airs, calcific, or bony densities.

**Results:** There were 42 (46.7%) malignant SPN and 48 (53.3%) benign SPN, which were grouped into A (18 tuberculoma, 13 fungus), B (5 focal organizing pneumonia, 5 abscess), and C (7 other benign tumors). The malignant SPN showed significantly higher mean attenuations of enhancement and net-enhancement than all benign SPN ( $P < 0.001$ ). Using the area under the receiver operating characteristic curve (AUC), the cut-off net-enhancement of 15 HU gave 83% sensitivity, 65% specificity and 73% accuracy for predicting malignancy. Malignant SPN (mean 67.9 HU) had significantly higher enhancement than group A (mean 52.6 HU,  $P < 0.001$ , 95% CI: 8.73, 21.81) and group B (mean 57.0 HU,  $P = 0.025$ , 95% CI: -1.43, 20.34) while group C showed no significant difference (mean 68.1 HU,  $P = 0.97$ ). Net enhancements were higher in group B (mean 18.8 HU) than in group A (mean 8.8 HU) ( $P < 0.001$ , 95% CI: 11.8, 23.18).

**Conclusions:** The semi-automated ROI measurement of SPN's attenuations on CT is an accurate approach in distinguishing indeterminate SPN.

**Keywords:** Solitary pulmonary nodule (SPN); lung carcinoma; sensitivity and specificity; computed-tomography

Submitted Sep 14, 2018. Accepted for publication May 07, 2019.

doi: 10.21037/jtd.2019.05.56

View this article at: <http://dx.doi.org/10.21037/jtd.2019.05.56>

## Introduction

Radiologically indeterminate solitary pulmonary nodules (SPN) on chest CT images often pose a challenge to radiologists in establishing a benign or malignant diagnosis.

In a similar respect, SPN found on clinical routine practice settings, regardless of their frequency, are never be underestimated; A recent study demonstrated that 12.4% of the SPNs detected in routine chest CT was lung cancer (1).

**Table 1** Characteristics of the patients and SPN

Patient	Malignant SPN	Benign SPN
Number [%]	42 [47]	48 [53]
Mean age (range)	66.8 (42 to 84)	57.7 (27 to 81)
Sex (male: female)	29:13	24:24
Size, cm (range)	2.7 (0.7 to 3.0)	2.5 (0.4 to 3.0)
Diagnosis	Primary lung cancer (n=36)	Tumor (n=7)
	Adenocarcinoma (n=24)	Hamartoma (n=3)
	Squamous cell carcinoma (n=6)	Sclerosing hemangioma (n=3)
	Small cell carcinoma (n=3)	Inflammatory pseudotumor (n=1)
	Carcinoid sarcoma (n=1)	Tuberculoma (n=18)
	Carcinoid (n=1)	Fungal infection (n=13)
	Lymphoma (n=1)	FOP* (n=5)
	Metastasis (n=6)	Abscess (n=5)

\*, focal organizing pneumonia.

For this reason, there have been many studies on evaluating malignant characteristics of SPN (2-7). It is well known that CT diagnostic analysis for predicting likelihood of malignancy of SPN is based on the lesion's size, growth, morphology and attenuation. Notable studies by Swensen *et al.* (2,3) showed that SPN's net enhancement of 15 HU or more correlates with malignancy.

In routine clinical settings, the CT density measurement is usually measured manually by drawing region of interest (ROI) in most of soft tissue of the lesion. However, manual analysis falls into subjective interpretation bias and such measurement may not truly reflect the entire lesion's enhancement patterns. Also, SPN with various sizes, margins and internal characteristics such as calcification, fat, air and fluid could further make the measurement a difficult process. The present study included the entire SPN for measuring ROI by semi-automated method with preset range of threshold attenuations.

The goal of the present study was to measure attenuation of various SPN beyond the scope of well-known SPN criteria using semi-automated ROI selection and subsequently determining sensitivity, specificity and accuracy for predicting malignancy.

## Methods

This retrospective study was approved by the institutional review board of our institution with a waiver of the

requirement for informed consent of the patients.

### Study population

A total of 115 patients with SPN detected on initial chest CT scans at our institution during 2 years were retrospectively reviewed. Peripheral lung nodules, compatible with lung-RAD, or Fleischer's society definition for SPN were chosen in this study. Finally, CT scans of ninety patients [56 men (63±12 years) and 34 women (62±11 years)] were reviewed by three thoracic radiologists (Y Choi, BM Gil and MH Chung, each with 2, 5 and 25 years of experience in thoracic imaging, respectively) via Picture Archiving and Communication System (PACS). SPN were defined as variable-sized (0.4–3.0 cm) solitary nodules of any shape located within lung parenchyma. The patient demographics findings are summarized in *Table 1*.

### Image acquisition and semi-automated CT ROI selection

SPN with various shapes and internal contents (rounded, lobulated and cavitary) on CT scans were included. Nodules containing benign-looking calcifications were excluded while those with stippled and peripheral small calcifications, uncertain low density areas or even small and large air cavities were included because any attenuation above 200 HU and below -100 HU (calcification, bony component and air) were automatically eliminated and only the remaining soft

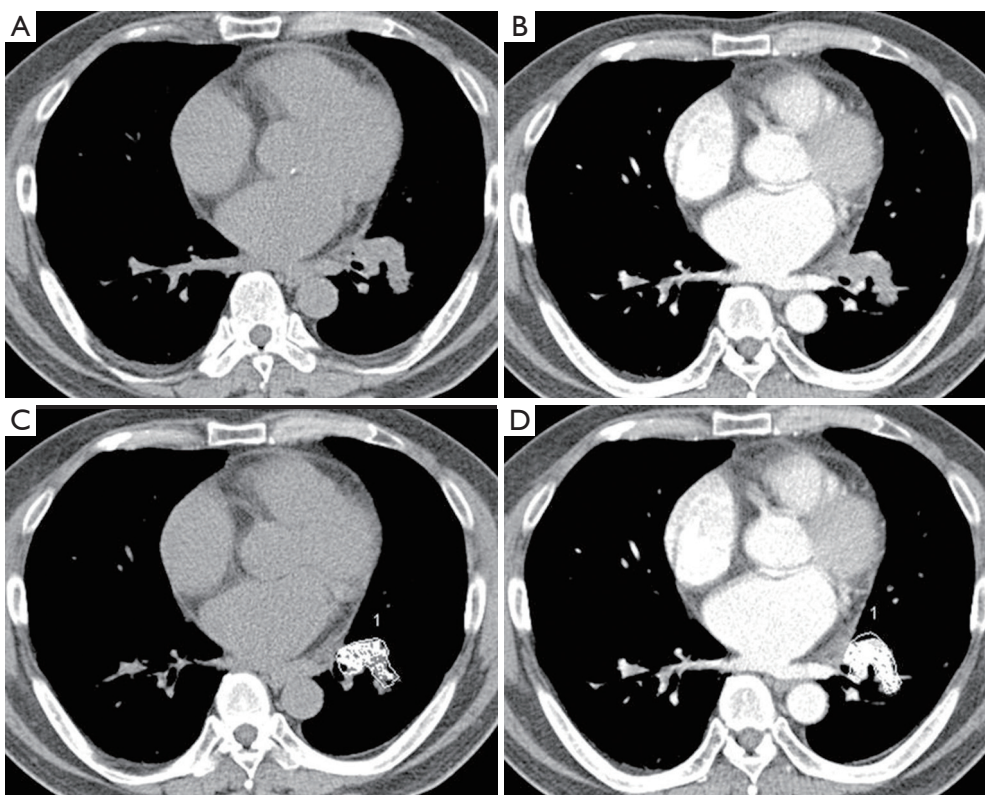


**Figure 1** Pre- (A) and post-enhanced CT (B) shows an irregular mass about 3.1 cm × 1.7 cm in the left lower lobe. Manual ROI drawing is not easy in the whole lesion site. But, by applying of ROI range from -100 to 200 HU (soft tissue density including necrosis, fat, hemorrhage and even microvessel, but not calcification, air), tumor is automatically drawn (white color areas) on (C) (PreE) and (D) (PostE) images. The mean density of the tumor (carcinoid) is about 38 HU on PreE CT and 55 HU on PostE CT (NetE; about 17 HU). Siemens, Lung Parenchyma Analysis. ROI, region of interest.

tissue components including fat and necrotic densities were measured by our method.

A 64-slice MDCT scanner (SOMATOM Sensation 64, Siemens Medical Solution, Forchheim, Germany) was used in 54 patients and a 128-slice MDCT (Discovery CT 750 HD, GE Medical Systems, Waukesha, WI, USA) was used in the rest of 36 patients with SPN. All CT scans were obtained with a 3-mm collimation at 3-mm intervals using a tube voltage of 120 kV and tube current of 130 mA covering the apices of the lungs to the pleural recesses. All chest MDCT images were reconstructed with the lung window settings (width, 1,000 to 1,500 HU; center, -700 HU) and with the mediastinum settings (width, 350 HU; center, 50 HU). Post-enhanced scan was obtained 70 seconds after contrast media (Ultravist, Shering, Berlin, Germany) injection; 120 mL of contrast media was injected at a rate of 2.0 mL/s using a power injector (MEDRAD, Stellant, Bayer, Leverkusen, Germany) without subsequent flushing with normal saline.

All patients were in supine position at full inspiration during all CT scans, which approximately took 3 minutes. All reconstructed MDCT images were transferred to workstations for quantitative assessment.

The transferred raw data images were analyzed by the three thoracic radiologists at the dedicated two workstations with software (GE AW area histogram, General Electrics, Fairfield, CT, USA; and Siemens, Lung Parenchyma Analysis, Siemens Medical Solution, Forchheim, Germany) that are programmed with algorithms for the automatic ROI assessment.

The ROIs of non-enhanced and contrast-enhanced CT images were roughly drawn peripherally around SPN, because surrounding lung airs were automatically eliminated. A predetermined range of densities (minimum: -100 HU, maximum: 200 HU) was entered into the software in order to eliminate calcifications and air allowing selective measurement of soft tissue densities. The ROIs included the entire SPN regardless of its shape or internal contents (*Figure 1*).

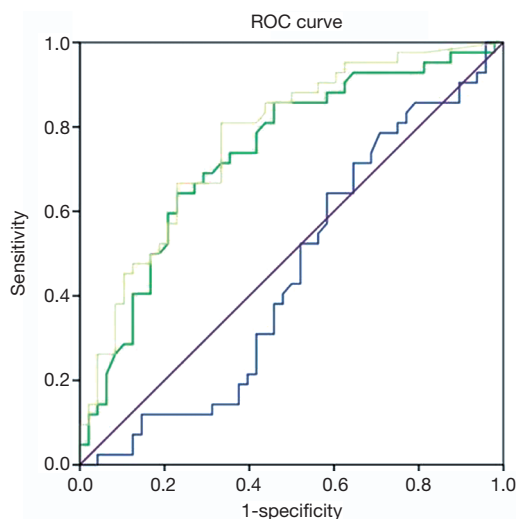


**Figure 2** ROC curve of SPN attenuations in PreEA (blue), EA (green) and NetEA (yellow) in all samples. EA and NetEA show meaningful curves with area under curve of 0.74 and 0.77, respectively. ROC, receiving operator characteristic; SPN, solitary pulmonary nodule.

The procedure for semi-automated ROI selection of SPN using Siemens and GE AW software included freehand ROI drawn on entire SPN. The pre-enhanced attenuation (PreEA) is the ROI value of SPN on the non-enhanced CT image and the enhanced attenuation (EA) is the ROI value of SPN on the contrast-enhanced CT image. Net-enhanced attenuation (NetEA) is the value of EA minus that of PreEA.

### Statistical analysis

Statistical analyses were performed using commercially available SPSS software for Windows (version 19.0; IBM Corp., Armonk, NY, USA). Continuous variables were presented as mean  $\pm$  standard deviation (SD). Mann-Whitney U test were used for comparing statistically significant differences in mean attenuations of PreEA, EA and NetEA between malignant and benign SPN. A P value  $<0.05$  was considered to be significant. We computed a receiving operator characteristic (ROC) curve to derive sensitivity, specificity, and accuracy for predicting SPN's malignancy (Figure 2).

## Results

There were 84 pathologically proven cases, 55 CT-guided

biopsy and 29 video-assisted thoracoscopic surgery (VATS) while the rest 6 cases were diagnosed by clinical observation such that no interval change of the SPN over two years of follow-up CT scans was considered benign. The prevalence of malignancy was 47% (42/90). The cell type of malignant tumors are as follows; 24 adenocarcinoma, 6 squamous cell carcinoma, 3 small cell carcinoma, 1 carcinoid tumor, 1 pleomorphic carcinoma, 1 lymphoma, and 6 metastatic tumors. The 48 benign lesions (53%) had various diagnoses and were grouped based on their nature (A: 18 tuberculoma, 13 fungus; B: 5 focal organizing pneumonia (FOP), 5 abscesses; C: 7 benign tumors). Within benign tumors, there were 3 hamartomas, 3 sclerosing hemangiomas, and 1 inflammatory pseudotumor (Table 1).

### Attenuations of SPN

The malignant SPN's attenuations after contrast enhancement (EA) ranged from 28.6 to 98.0 HU and benign SPN's EA from 18.3 to 86.8 HU. The mean attenuations of PreEA, EA, and NetEA of malignant SPN were  $43.6 \pm 11.5$ ,  $67.9 \pm 14.0$  and  $26.3 \pm 13.4$  HU, respectively. The mean attenuations of PreEA, EA, and NetEA of benign SPN were  $26.3 \pm 13.4$ ,  $55.9 \pm 14.5$ , and  $13.3 \pm 12.2$  HU. The EA and NetEA of malignant SPN were significantly higher than those of the entire benign A–C groups (EA  $t=4.00$ ,  $P<0.001$ ; NetEA  $t=4.43$ ,  $P<0.001$ ) (Table 2). The cut-off EA of 61 HU or more gave 73.8% sensitivity, 62.5% specificity, 63% PPV, 77% NPV and 69% accuracy. The cut-off NetEA of 15 HU or more gave 83% sensitivity, 65%, specificity, 67% PPV, 82% NPV and 73% accuracy. Malignant SPN (mean 67.9 HU) had significantly higher enhancement than group A (mean 52.6 HU,  $P<0.001$ , 95% CI: 8.73, 21.81) and group B (mean 57.0 HU,  $P=0.025$ , 95% CI: -1.43, 20.34) whereas group C showed no significant difference (mean 68.1 HU,  $P=0.97$ ). Net enhancements were higher in group B (mean 18.8 HU) than in group A (mean 8.8 HU) ( $P<0.001$ , 95% CI: 11.8, 23.18) (Table 3).

### ROC curve

ROC curve was plotted for attenuations in PreEA, EA and NetEA of all samples. EA and NetEA showed meaningful curves for sensitivity and specificity (Figure 2).

## Discussion

Thoracic radiologists routinely encounter SPN of various

**Table 2** Comparison of attenuations of PreEA, EA, and NetEA between malignant and benign SPN

CT attenuation	Malignant group	Benign group (total)	P
PreEA			0.369
Mean	43.6±11.5	26.3±13.4	
Median (range)	41.1 (23.1, 65.1)	42 (15, 66.2)	
EA			<0.001
Mean	67.9±14.0	55.9±14.5	
Median (range)	70.3 (28.6, 98)	53.9 (18.9, 85.9)	
NetEA			<0.001
Mean	26.3±13.4	13.3±12.2	
Median (range)	26.5 (0, 62.8)	10.6 (0, 44.8)	

PreEA, pre-enhanced attenuation; EA, enhanced attenuation; NetEA, Net-enhanced attenuation value of EA minus that of PreEA.

**Table 3** Comparison of mean attenuation of PreEA, EA, and NetEA among three benign groups

CT attenuation	Malignant	Benign group A	P (95% CI)	Benign group B	P (95% CI)	Benign group C	P*
PreEA	43.6±11.5	45.4±12.9	0.151 (−8.76, 1.38)	38.5±6.0	0.269 (−2.49, 8.73)	43.9±10.3	0.528
EA	67.9±14.0	52.6±13.4	<0.001 (8.73, 21.81)	57.0±13.6	0.025 (−1.43, 20.34)	68.1±15.8	0.967
NetEA	26.3±13.4	8.8±9.5	<0.001 (11.8, 23.18)	18.8±13.3	0.105 (−1.62, 16.57)	24.1±11.5	0.644

\*, non-parametric statistical comparison (Mann-Whitney U test) between malignant and benign group C was used. Including the only pathology proven nodules (group A: 28; group B: 8; group C: 6). PreEA, pre-enhanced attenuation; EA, enhanced attenuation; NetEA, EA-PreEA.

sizes, shapes and densities on CT scans. Making use of CT enhancement patterns of such indeterminate SPN could aid in diagnosis and patients would benefit from reduced cost and radiation dose caused by additional follow-up CT scans and invasive procedures like CT-guided biopsy or VATS.

Since Swensen *et al.* (2,3) emphasized that absence of significant lung nodule enhancement values 15 HU or less at CT is strongly predictive of benignity, various threshold attenuation values have been reported to be useful for distinguishing malignant nodules from benign nodules at contrast-enhanced dynamic CT with single- or multi-detector row helical machines (4-7). This enhancement cutoff of 15 HU resulted in an excellent sensitivity of 98% but it only had 58% specificity. The general conclusion based on this report was that benign lesions usually enhance no more than 15 HU, whereas most of the malignant nodules develop more intensive enhancement, usually over 20 HU (7). On the other hand, Yi *et al.* reported that with 30 HU or more of net enhancement as a cutoff value in differentiation of malignant and benign nodules, sensitivity for malignant nodules was 99%, specificity was

54%, and accuracy was 78% (6). Malignant nodules showed significantly higher maximum relative enhancement ratio, shorter time to peak enhancement (6). Most malignant nodules had peak enhancement approximately two minutes after the administration of contrast media. In this study, the mean peak enhancement (MPE) of malignant nodules was reaching 98 HU, whereas relatively previous articles reported the MPE was approximately 40 HU (range, 41.9–46.5 HU) (8). In the more recent study, the evaluation of SPNs using dynamic contrast-enhanced MDCT was conducted by analyzing combined criteria for malignancy including wash in of contrast medium of 25 HU or greater and washout of 5–31 HU on 15 minutes-delayed imaging (4). The result of this study shows high sensitivity (94%), specificity (90%) and accuracy (92%) for detection of malignancy.

We used semi-automated ROI measurement method for more accurate attenuation measurement in order to differentiate malignant from benign SPN. In our study, EA and NetEA of malignant SPN were significantly higher than those of the benign group (enhancement  $t=4.00$ ,  $P<0.001$ ;

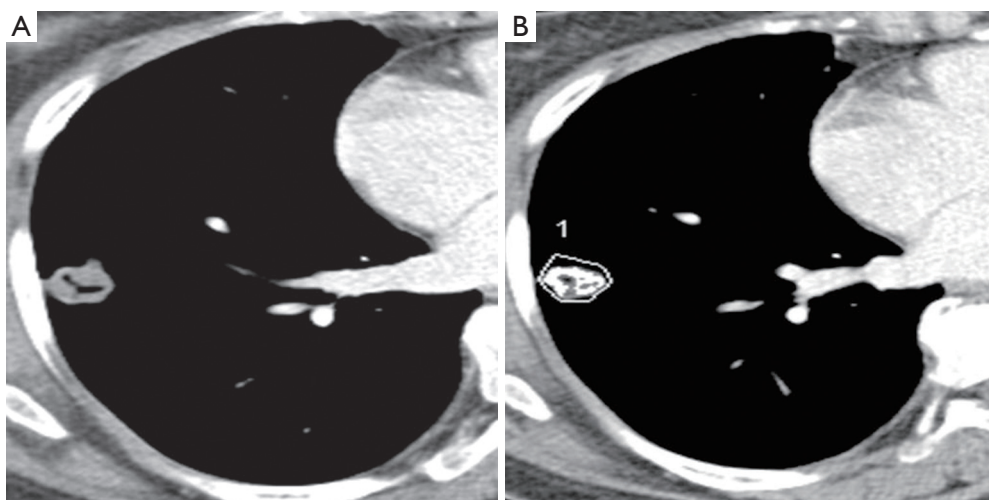


**Figure 3** Measurement of SPN attenuations (Siemens, Lung Parenchyma Analysis). (A) After contrast injection without ROI selection; (B) after contrast injection with ROI selection, using Lung Parenchyma Analysis. Free hand ROIs are applied roughly peripherally around SPN so that internal air cavity is automatically eliminated. This lesion was diagnosed as tuberculoma and did not enhance at all (B: 37.6 HU C: 37.7 HU). ROI, region of interest; SPN, solitary pulmonary nodule.

net enhancement  $t=4.43$ ,  $P<0.001$ ), and the optimal cut-off NetEA of 15 HU or more yielded acceptable sensitivity (83%), specificity (65%) and accuracy (73%) for predicting malignant potential of SPN as compared with previous studies mentioned above. Our specificity was not low compared to the Swensen *et al.* and the accuracy was similar in comparison with the Yi *et al.* However, the reason for the subtle differences is probably that our study did not use dynamic CT. Second reason may be different measurement method itself between manually selected ROI and automatic total ROI. Third reason is likely to include too small nodules and heterogeneous nodules such as cavitory tuberculoma (Figure 3), necrotic lung cancer (Figure 4), or lung abscess. This is a kind of preliminary reports of small populations.

One study demonstrated solid non-calcified pulmonary nodules larger than 5 cm and their irregular, spiculated or lobulated margin increased the likelihood of nodule's malignancy, whereas nodule density had no discriminative power; however, in contrast to our study, their density measurement of pulmonary nodules included air or air-bronchogram and hemorrhage within the tumor thus giving a wide range of densities (9). Our study used pre-determined range of densities from -100 to 200 HU in order to selectively measure only the solid enhancing portion of SPN because this range is a zone of soft tissue density area including cystic, necrotic, fatty portions, even

hemorrhagic areas, but not calcifications, bony components, and airs. Indeed, our attempt is to eliminate the just calcific (almost benignity; about higher than 200 HU) or air densities (necrotic air cavity; about -1,000 HU) because of these materials are major errors of nodule homogeneity. There are also other advantages in segmentation of nodules by defining this range (from -100 to 200 HU). We can measure nodules in any size or shape even if we draw roughly outer periphery of nodule including the regional normal lung fields, because the surrounding lungs (about over -700 to 800 HU) are automatically eliminated (Figure 5). Sometimes, some pixels, which were just soft tissues, but not calcific or airs, were not covered as white figures on Lung Parenchyma Analysis (Siemens) (Figures 1,3). We are not sure the reason why. But we suppose that those areas are beyond 200 HU such as microcalcifications, highly vascularized areas or microvessel.

In addition to evaluating SPN's malignant potential compared to all kinds of benign nodules, the present study described EA and NetEA of various benign SPN (tuberculoma, fungus, FOP, abscess and benign tumors) (Figures 6,7) independently and compared with malignant nodules. In our study, malignant SPN had significantly higher NetEA than that of group A (tuberculoma and fungus) and group C (benign tumor) while group B (FOP and abscess) showed no significant difference. Previous study by Zhang *et al.* demonstrated positive correlation

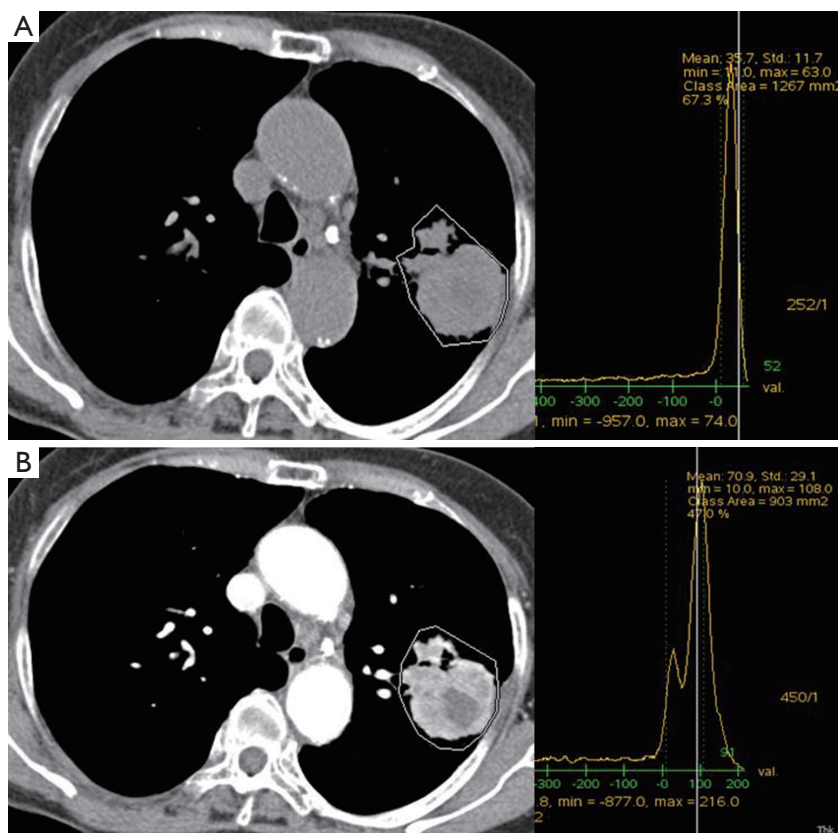


**Figure 4** GE AW area histogram software measuring ROI of irregularly shaped SPN with heterogeneous internal contents with respective attenuation histograms (A) before contrast injection and (B) after contrast enhancement; enhanced attenuation: 70.9 HU, net enhancement: 35.2 HU. The final diagnosis was found out to be non-small cell lung cancer. ROI, region of interest; SPN, solitary pulmonary nodule.

between enhancement and vascularity within lung carcinoma, inflammatory pseudotumor, and tuberculoma in order of higher enhancement (10). Our findings in this study are consistent with the concept that malignant SPN expresses tumor angiogenesis and enhance stronger than the benign counterpart (11). As expected, the mean values of EA and NetEA of malignant SPN were significantly higher than those of benign SPN. In addition, the optimal cut-off NetEA value of 15 HU or more for distinguishing malignant from benign SPN, especially chronic granulomatous lesions, gave acceptable range of sensitivity, specificity and accuracy that are reasonably consistent with previous studies. There was no significant NetEA difference between malignant and benign group B (FOP, abscess) SPN. No significant difference in EA was found between malignant SPN and group B and C. Like this, the results of our study between malignant and FOP and abscess was relatively corresponded to those of previous study (4). They

reported that malignant and some non-specific benign nodules showed persistent enhancement without washout. In fact, we experienced in clinical fields that many FOP, abscess wall and some benign tumor such as sclerosing hemangioma are nearly similar to malignant tumor in point of view of enhancement pattern. Hittmair and Zhang found similar results in that benign pulmonary nodules of inflammatory nature displayed strongest enhancement (12,13). Upon encountering such SPN, considering other parameters of malignancy such as large size, spiculated or lobulated margin and interval growth could help in correct diagnosis.

CT assessment was most effective for lesions 2.0 cm or less in diameter (14). Small solid-density pulmonary adenocarcinoma has poor prognosis even if they are less than 2.0 cm in size (15). Other studies limited selection of SPNs to 5 mm to 3 cm in diameter with homogeneous density of spherical shape without cavitation, necrosis,

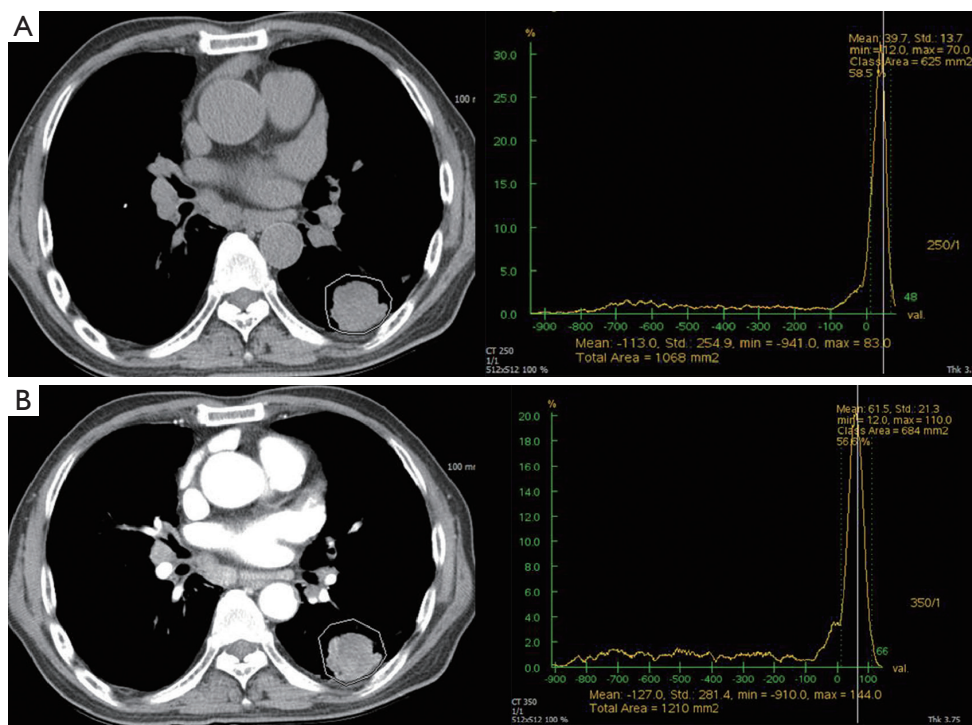


**Figure 5** A good demonstration of measuring attenuation of SPN on enhanced CT suspected of malignancy (finally, carcinosarcoma) in left lower lobe (A, left) before and (B, left) after contrast enhancement (CM). Free hand ROI selection, using GE AW area histogram, is shown on (A, right) and (B, right) images. SPN, solitary pulmonary nodule; ROI, region of interest.

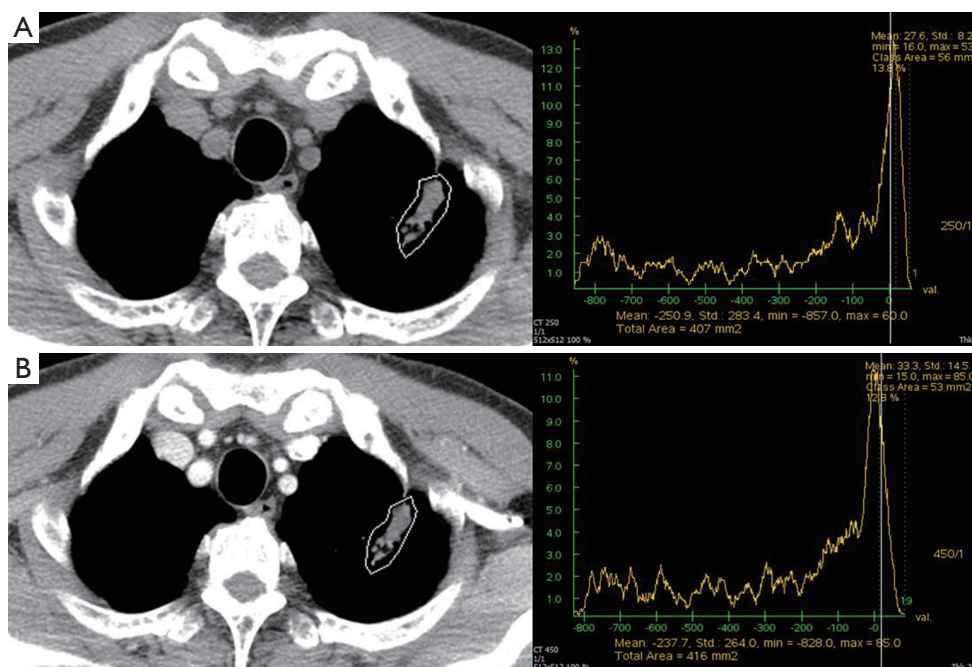


**Figure 6** An irregular, elongated non-calcific nodule is seen in left apical segment on PreE CT (A). This free hand ROI is about mean 27.7 HU. After enhancement (B), CT shows little enhancing lesion about mean 33.3 HU (NetE; about 5.6 HU). It turned out to tuberculoma.

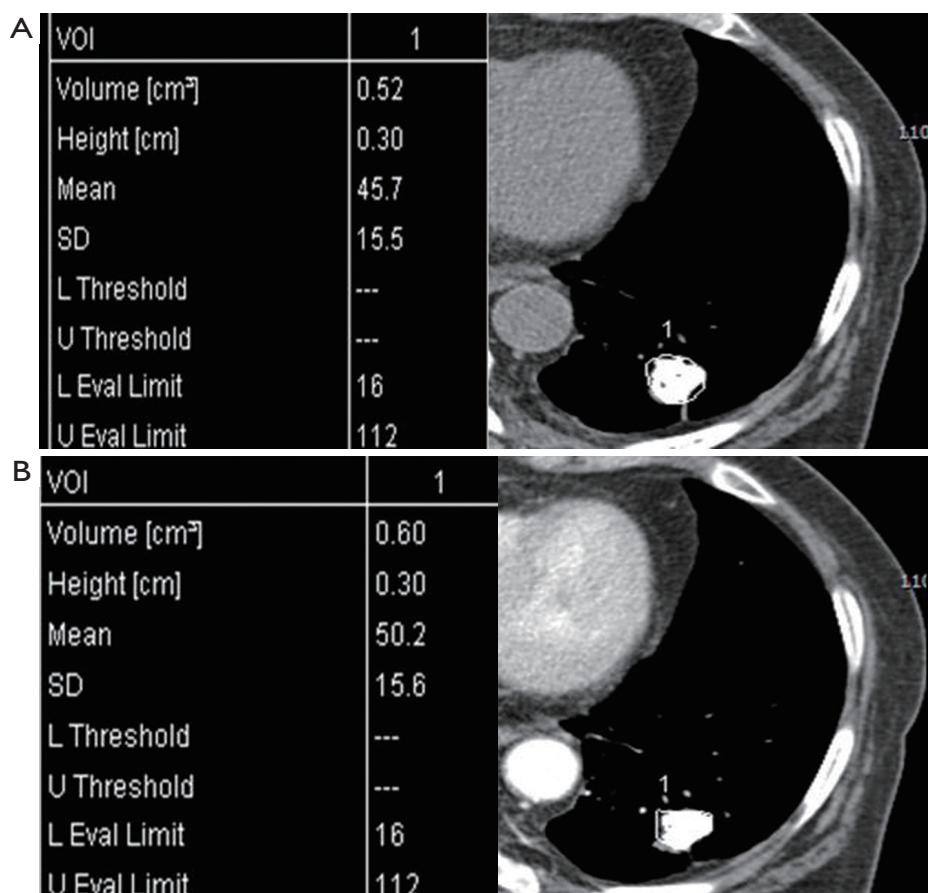


**Figure 7** Pre-enhanced CT (A) shows an irregular, 2.0 cm-sized nodule with thin pleural tail in left lower lobe. On post-enhanced CT (B), a nodule was poorly enhanced. Free hand ROI was drawn as white figures on (A,B). Mean density of nodule was about 45.7 HU on PreE (A) and 50.2 HU on PostE (B) with 4.5 HU NetE. Operation pathology was aspergilloma. ROI, region of interest.

calcifications and fat because this criterion allows for optimal manual measurement of central ROI (2,7). Even for larger SPN, internal cavitation and air-bronchogram are CT features frequently associated with malignancy and manual selection of solid portion in mixed densities may not be an easy task (16,17). Using semi-automated ROI measurement, our study was able to include SPN of any sizes from small to large and of various internal contents via comprehensive inclusion of solid portion of SPN under a preset range of densities. The mean values of our results in both malignant and benign nodules tend to be lower than those of previous reports. The reason for this phenomenon was that our semi-automated method included all heterogeneous necrotic portions of solid tumors, whereas previous manual methods excluded non-solid low-density areas involuntarily.

There are several limitations that we need to address.

First, the study's retrospective nature is prone to selection bias. The number of total samples was relatively small ( $n=90$ ) which is subject to lower statistical power. With respect to technical aspects, the two CT scanners used different software but we assumed their algorithm and ability to measure attenuation were probably the same. All contrast-enhanced CT images were acquired 70 seconds after contrast injection which might have led to variations related to patients' breath holding. However, we assumed contrast media enter the bronchial arteries in 11–19 seconds and more than half of contrast would have reached extravascular space of most tissues in 60 seconds (18). However, we wanted all CT data to be as similar to clinical settings as possible and for that reason, dynamic contrast-enhanced CT scan wasn't applied for this study. Finally, all CT scans were sliced at 3-mm thickness, which could have neglected ground-glass elements.

## Conclusions

In conclusion, our study demonstrated a novel approach in measuring attenuation of SPN of various sizes, shapes and internal contents. Compared with similar previous studies on SPN density measurement, we showed similar sensitivities and specificities in predicting malignancy thereby proving the applicability of semi-automated ROI measurement on CT in evaluating SPN to a larger extent.

## Acknowledgments

None.

## Footnote

*Conflicts of Interest:* The authors have no conflicts of interest to declare.

*Ethical Statement:* The study was approved by institutional review board of our institution (Bucheon St. Marys Hospital) (No. HC16RASI0101) and written informed consent was obtained from all patients.

## References

- Gómez-Sáez N, Hernández-Aguado I, Vilar J, et al. Lung cancer risk and cancer-specific mortality in subjects undergoing routine imaging test when stratified with and without identified lung nodule on imaging study. *Eur Radiol* 2015;25:3518-27.
- Swensen SJ, Viggiano RW, Midthun DE, et al. Lung nodule enhancement at CT: multicenter study. *Radiology* 2000;214:73-80.
- Swensen SJ, Brown LR, Colby TV, et al. Lung nodule enhancement at CT: prospective findings. *Radiology* 1996;201:447-55.
- Jeong YJ, Lee KS, Jeong SY, et al. Solitary pulmonary nodule: characterization with combined wash-in and washout features at dynamic multi-detector row CT. *Radiology* 2005;237:675-83.
- Schaefer JF, Vollmar J, Schick F, et al. Solitary pulmonary nodules: dynamic contrast-enhanced MR imaging--perfusion differences in malignant and benign lesions. *Radiology* 2004;232:544-53.
- Yi CA, Lee KS, Kim EA, et al. Solitary pulmonary nodules: dynamic enhanced multi-detector row CT study and comparison with vascular endothelial growth factor and microvessel density. *Radiology* 2004;233:191-9.
- Choromańska A and Macura KJ. Evaluation of solitary pulmonary nodule detected during computed tomography examination. *Pol J Radiol* 2012;77:22-34.
- Yamashita K, Matsunobe S, Tsuda T, et al. Solitary pulmonary nodule: preliminary study of evaluation with incremental dynamic CT. *Radiology* 1995;194:399-405.
- Xu DM, van Klaveren RJ, de Bock GH, et al. Limited value of shape, margin and CT density in the discrimination between benign and malignant screen detected solid pulmonary nodules of the NELSON trial. *Eur J Radiol* 2008;68:347-52.
- Zhang Z, Zhang C, Wu P, et al. Comparison of enhanced thin CT sections with pathologic findings in pulmonary carcinoma, inflammatory, pseudo-tumor and pulmonary tuberculoma. *Zhonghua Zhong Liu Za Zhi* 2002;24:173-7.
- Tateishi U, Nishihara H, Watanabe S, et al. Tumor angiogenesis and dynamic CT in lung adenocarcinoma: radiologic-pathologic correlation. *J Comput Assist Tomogr* 2001;25:23-7.
- Hittmair K, Eckersberger F, Klepetko W, et al. Evaluation of solitary pulmonary nodules with dynamic contrast-enhanced MR imaging--a promising technique. *Magn Reson Imaging* 1995;13:923-33.
- Zhang M, Kono M. Solitary pulmonary nodules: evaluation of blood flow patterns with dynamic CT. *Radiology* 1997;205:471-8.
- Siegelman SS, Khouri NF, Leo FP, et al. Solitary pulmonary nodules: CT assessment. *Radiology* 1986;160:307-12.
- Ikehara M, Saito H, Kondo T, et al. Comparison of thin-section CT and pathological findings in small solid-density type pulmonary adenocarcinoma: prognostic factors from CT findings. *Eur J Radiol* 2012;81:189-94.
- Gadkowski LB, Stout JE. Cavitory pulmonary disease. *Clin Microbiol Rev* 2008;21:305-33.
- Onn A, Choe DH, Herbst RS, et al. Tumor cavitation in stage I non-small cell lung cancer: epidermal growth factor receptor expression and prediction of poor outcome. *Radiology* 2005;237:342-7.
- Littleton JT, Durizch ML, Moeller G, et al. Pulmonary masses: contrast enhancement. *Radiology* 1990;177:861-71.

**Cite this article as:** Choi Y, Gil BM, Chung MH, Yoo WJ, Jung NY, Kim YH, Kwon SS, Kim J. Comparing attenuations of malignant and benign solitary pulmonary nodule using semi-automated region of interest selection on contrast-enhanced CT. *J Thorac Dis* 2019;11(6):2392-2401. doi: 10.21037/jtd.2019.05.56